Available online at www.sciencedirect.com

ScienceDirect

Procedia Manufacturing 8 (2017) 345 – 352

Procedia MANUFACTURING

14th Global Conference on Sustainable Manufacturing, GCSM 3-5 October 2016, Stellenbosch, South Africa

Comparative Characterization of P91 and 10CrMo9-10 Creep Resistant Steel Welds

D. M. Madyira[a*], J. A. Liebenberg[a], A. Kaymacki[a]

[a]*Department of Mechanical Engineering Science, University of Johannesburg, Auckland Park 2006, Johannesburg*

Abstract

P91 and 10CrMo9-10 creep resistant steels are critical to the performance of boiler tubes and power generating plants in general. Components made from these materials are mainly joined by welding. This paper reports on the comparative study of the effect of TIG and SMAW welding on the mechanical performance of P91 and 10CrMo9-10. TIG was used for root welding while SMAW was used for weld filling of V-butt joints. Specimens of the two alloys prepared using recommended welding procedures are evaluated using optical microscopy and Vickers micro hardness assessment. Some specimens were post weld heat treated while others were not. Post weld heat treated (PWHT) specimens exhibited similar properties as the corresponding base materials for both steels. TIG welding resulted in significant grain size reduction in both steels. PWHT produced more consistent grain structure, which is favorable.

Peer-review under responsibility of the organizing committee of the 14th Global Conference on Sustainable Manufacturing

Keywords: P91; 10CrMo9-10; Microhardness, Tungsten Inert Gas Welding, Shieled Metal Arc Welding

1. Introduction

The use of creep resistant steels for the fabrication of components such as boiler tubes and fittings in power generation plants due to their high temperature strength properties has become the norm in recent years. The fabrication and repair of these components has however led to challenges regarding the degradation of mechanical properties and the formation of undesirable microstructures in the welded steels. The operating conditions of creep resistant steels induce large thermal and mechanical stresses on these components. Creep resistant steels such as P91 and 10CrMo9-10 are introduced due to their attractive mechanical performance at elevated temperatures, especially creep resistance [1]. These properties depend on the chemical composition and microstructure of the steel. In order to manufacture and repair the various components using these materials, permanent joining through fusion welding

Peer-review under responsibility of the organizing committee of the 14th Global Conference on Sustainable Manufacturing
doi:10.1016/j.promfg.2017.02.044

processes is required [2], [3]. Welding in this case is a necessary compromise since no other fabrication process will be as cost effective or practical. The various effects of intense heat during welding on the microstructure of creep resistant steels, the inclusion of filler material in the weld joints, the formation of heat affected zones (HAZ) and post weld heat treatments (PWHT) have been shown to have an impact on the mechanical and thermal performance of creep resistant steel weldments [4]. The HAZ formed from the welding process has been shown to be a problematic area due to the development of crack defects in the weldment leading to failure [5]. The challenges faced with the welding of steels such as P91 and 10CrMo9-10 has therefore led to the need for an investigation into the mechanical property changes and microstructural evolution of welded P91 and 10CrMo9-10 steels as a result of thermal exposure during welding.

2. Methodology

2.1. Aims of Experiment

The aim of this investigation of P91 and 10CrMo9-10 steel welding was to determine the effects of the welding on the mechanical performance of P91 and 10CrMo9-10.

2.2. Material Properties

P91 is normal 9CrMo steel modified by the addition of creep enhancing vanadium. This makes P91 an optimal material for high temperature high stress applications [6]. The second steel investigated was 10CrMo9-10 steel, which is a low alloy steel containing only 2.25% chromium as compared to the 9% of P91 steel [7]. The chemical composition for P91 and 10CrMo9-10 used in this investigation are presented in Tables 1 and 2 respectively.

Table 1. Chemical composition of P91

ELEMENT	C	Ni	N	Mn	Cr	Mo	V	Si	P	S	Al	Nb	Fe
WEIGHT	0.08-	<0.4	0.03-	0.3-	8-	0.85-	0.18-	0.2-	<0.02	<0.01	<0.04	0.06-	Bal.

Table 2. Chemical Composition of 10CrMo9-10

ELEMENT	C	Mn	Cr	Mo	Si	P	S	Fe
WEIGHT (%wt)	0.05-0.15	0.3-0.6	1.9-2.6	0.87-1.13	<0.15	<0.025	<0.025	Bal.

The typical mechanical properties of P91 and 10CrMo9-10 steel are presented in Table 3 [8].

Table 3. Mechanical properties of P91 and 10CrMo9-10

	Yield strength(MPa)	Tensile Strength(MPa)	Hardness(HV) (Tubes Only)
P91	415 min	630-830	190 min
10CrMo9-10	205 min	480-630	263 max

2.3. Sample Descriptions

The welded samples consisted of one P91-to-P91 weldment, and four 10CrMo9-10-to-10CrMo9-10 weldments. The P91 weldment had dimensions of 74.15 × 64.5 × 20.1 mm. The first welding procedure used on the P91 steel consisted of a TIG welding process to develop the joining root; the remainder of the V-groove joint was developed through SMAW/MMA welding. The remaining four 10CrMo9-10 samples were prepared solely through TIG welding to join two cylindrical steel tubes together. The dimensions of the 10CrMo9-10 tubes prepared is presented in Table 4.

Table 4. 10CrMo9-10 weldment descriptions

Sample	Outside Diameter(mm)	Wall Thickness(mm)	Welding Position
1	50	4.40	PH/5G
2	50	4.40	PC/2G
3	50	4.40	PH/5G
4	45	6.15	PH/5G

2.4 Equipment

The specimens were welded using a Multiarc 400 heavy duty multi-process welding machine, while the microstructural analysis and Vickers hardness testing were performed using an Olympus BX51M microscope and a TIME6301 digital Micro Vickers hardness tester respectively. The mentioned equipment is presented in Fig. 1 (a-c).

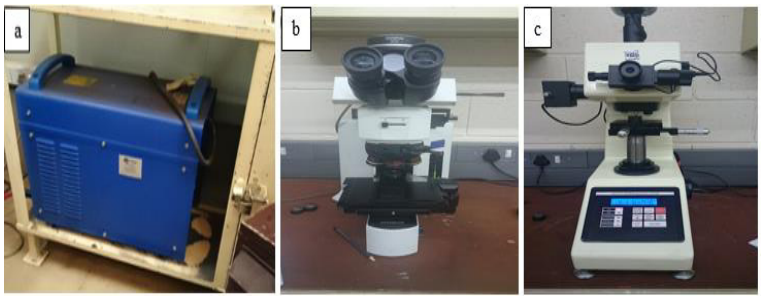

Fig. 1. (a) Multiarc 400 heavy duty multi process welding machine; (b) Olympus BX51M optical microscope; (c) TIME63014 digital micro vickers hardness tester

2.5 Experimental Procedure

All hardness tests were performed using a load of 2.94N with a dwell time of 15s.

2.5.1 10CrMo9-10

The hardness tests performed on the 10CrMo9-10 samples were taken across the weldment starting from the base metal to the HAZ and finally the fusion zone in 1mm increments. The hardness test results were also converted to tensile strengths to determine the impact of hardness on the tensile strength of the material.

2.5.2 P91

The size of the P91 sample allowed for multiple hardness tests to be performed at different heights. The P91 sample was marked at five different levels 15mm apart, the first being 0mm and the last being 60mm as shown in Fig. 2. At each level, 12 hardness tests were performed at 2mm increments towards the centre of the weld joint. The total hardness tests performed at the five levels resulted in 65 readings, leading to a 3D hardness profile.

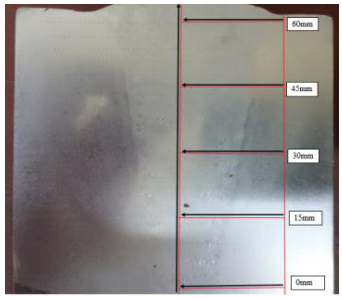

Fig. 2. P91 hardness test positions

3. Results and Discussion

3.1 10CrMo9-10 Microstructure Evolution

The grain structures of the 10CrMo9-10 samples exhibited similar structures in all cases. The TIG welding process resulted in a reduction in the grain size of the 10CrMo9-10 materials from the base metal to the fine grain heat affected zone (FGHAZ). This microstructure is shown in Fig. 3-6. The different weld zone microstructures for each sample are shown. The grain sizes in the coarse grain heat affected zone (CGHAZ) region were larger than those of the FGHAZ. The variation in grain size at the HAZ region from the FGHAZ to the CGHAZ was due to the heat input of the TIG welding process causing a solid phase transformation in the HAZ as a result of heating to austenitic temperatures triggering the FGHAZ to form fine grains. The coarse grains in the CGHAZ formed due to the formation of austenite grains during heating and different cooling rates than the FGHAZ. The CGHAZ does not see the formation of new grains, but instead retain their larger prior austenite grain sizes [9].

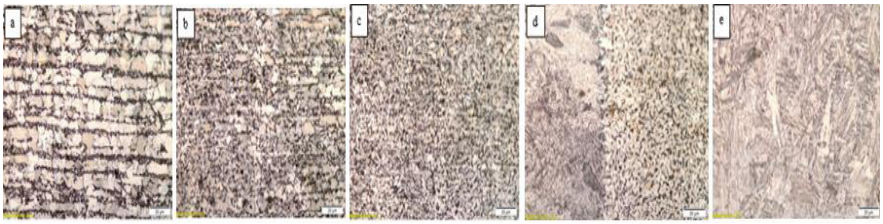

Fig 3. 10CrMo9-10 weldment sample one at 20x magnification (a) Base metal (b) Base metal to FGHAZ transition (c) HAZ (d) CGHAZ to Fusion zone transition (e) Fusion zone

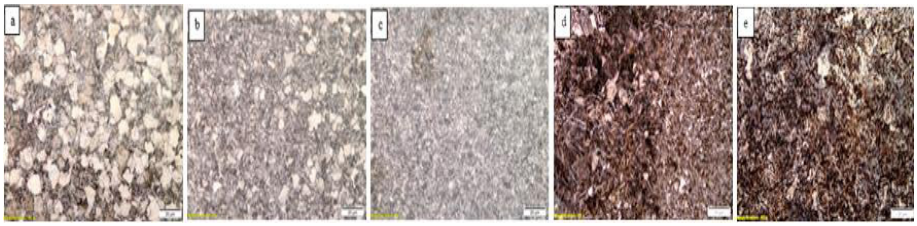

Figure 4. 10CrMo9-10 weldment sample two at 20x magnification (a) Base metal (b) Base metal to FGHAZ transition (c) HAZ (d) CGHAZ to Fusion zone transition (e) Fusion zone

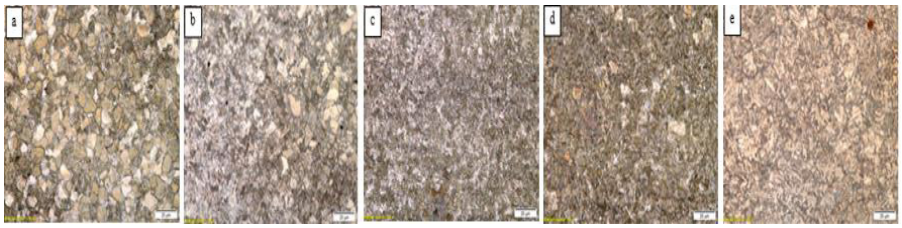

Figure 5. 10CrMo9-10 weldment sample three at 20x magnification (a) Base metal (b) Base metal to FGHAZ transition (c) HAZ (d) CGHAZ to Fusion zone transition (e) Fusion zone

All TIG welded samples had base metals with ferrite phase and carbide precipitation due to 10CrMo9-10 steels being bainite in nature [7]. The coarse bainite grain structure in the fusion zone that differs so greatly from the rest of the weldment may also be due to the lack of PWHT.

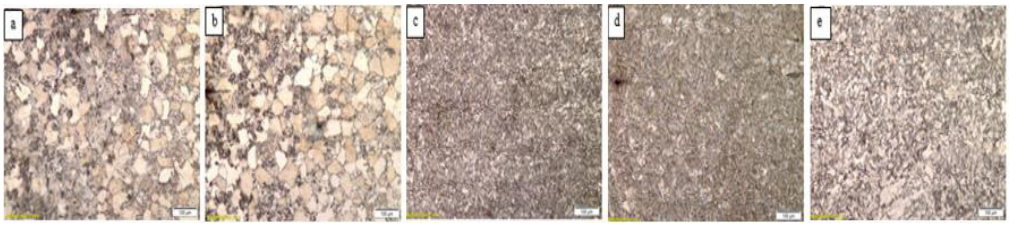

Figure 6. 10CrMo9-10 weldment sample four at 20x magnification (a) Base metal (b) Base metal to FGHAZ transition (c) HAZ (d) CGHAZ to Fusion zone transition (e) Fusion zone

3.2 P91 Microstructure Evolution

The microstructure of the welded P91 sample has distinct zones formed during the welding. These are visible in Fig. 7, which clearly illustrates the base material, HAZ and fusion zone. The P91 sample was PWHT, which resulted in a greater consistency of the microstructure phase throughout the weldment than that observed in the 10CrMo9-10 samples. In Figure 7 (a), the P91 base material can be observed. Due to post weld heat treatment, the base metal of the weldment was seen to have a tempered martensite structure. Following the weldment as it transitioned from the base material to the HAZ in Fig. 7(b), the change in microstructure transformed from the tempered martensite base metal microstructure to the tempered martensite FGHAZ with smaller grains. The HAZ experienced high temperatures for a short time below melting temperatures which resulted in the formation of fine grains in the HAZ due to solid state transformation.

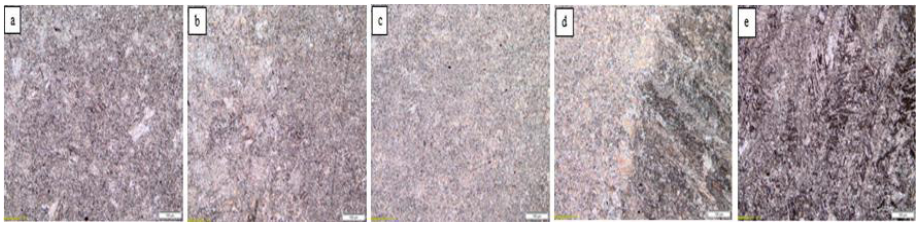

Fig. 7. P91 microstructure of different zones at 10x magnification; (a) Base metal; (b) Base metal to HAZ transition; (c) HAZ; (d) HAZ to fusion zone transition; (e) Fusion zone

The point at which the CGHAZ transitions to the fusion weld material was visible. The evolution of the microstructure is displayed in Fig. 7(c-d). Fig. 8 (a-b) show the transition from the base material to the FGHAZ from left to right. It was noticed that grain size decreased from the base material to FGHAZ. During the welding process, fewer precipitates were allowed to dissolve into the FGHAZ. This means that the martensite structure at the FGHAZ did not possess creep resistant properties as good as the rest of the weldment [10].

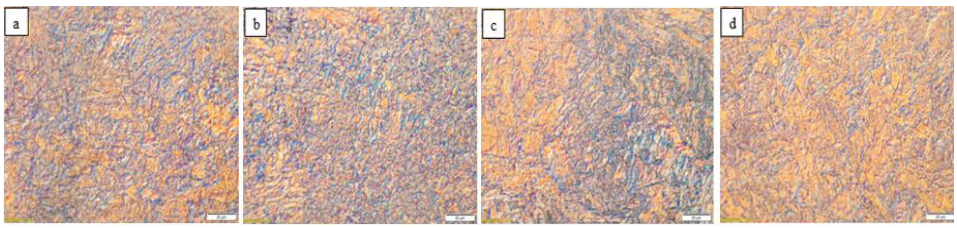

Fig. 8. P91 Microstructure at 50× magnification (a) Base metal (b) FGHAZ (c) CGHAZ (d) Fusion zone

In addition, the FGHAZ also experienced the formation of equiaxed grains at temperatures close to melting point. This grain refinement restricts the formation of strengthening precipitates at the grain boundaries of the PWHT P91 steel. This in turn leaves the FGHAZ vulnerable to type IV cracking [11]. The boundary between the

CGHAZ and the fusion zone could be seen by the devolvement of a more consistent grain structure in Fig. 8 (c). In Fig. 8 (d) the microstructure of the fusion zone consisting of a martensite microstructure can be seen, which closely resembles that of the base metal and highlights the effects of PWHT.

3.3 10CrMo9-10 Microhardness and Tensile Strength

The results of the 10CrMo9-10 microhardness tests presented a similar trend in all the weldments tested. As illustrated in Tables 5 and 6, there is a variation in hardness in the three distinct weld zones i.e. base metal, HAZ and fusion zones. The hardness profiles showed that the base metal had the lowest hardness value ranging from 150- 250 HV as expected for 10CrMo9-10. The estimated average tensile strength of the base metal lies in the range 542-606 MPa and conformed to the normal range of 480-630 MPa.

Table 5. Minimum and maximum hardness and tensile strength exhibited in the 10CrMo9-10 samples

	Min Hardness(HV)	Min Tensile Strength (MPa)	Max Hardness(HV)	Max Tensile Strength (MPa)
Sample 1	150	496	331	1039
Sample 2	176	589	384	1226
Sample 3	194	632	371	1173
Sample 4	1733	583	392	1249

The hardness measured in the HAZ displayed a significant increase with values well above 300 HV and tensile strength values exceeding 1000 MPa. The high hardness in the HAZ was due to the heat input during welding resulting in residual stresses in the weldments due to differential straining during heating and cooling.

Table 6. Average hardness and tensile strength in the 10CrMo9-10 weld zones

	Base Metal Average		Heat Affected Zone Average		Fusion Zone Average	
	Hardness(HV)	Tensile Strength (MPa)	Hardness (HV)	Tensile Strength (MPa)	Hardness (HV)	Tensile Strength (MPa)
Sample 1	162	542	270	861	271	862
Sample 2	184	612	337	1058	325	1024
Sample 3	250	800	347	1095	315	987
Sample 4	181	606	338	1076	319	1005

The hardness in the HAZ makes it an ideal location for type III and IV cracking which can negatively affect the mechanical performance of the 10CrMo-9-10 weldments in service. The hardness and tensile strength values of the fusion zone decreased from that observed in the HAZ but remained substantially higher than the base metal due to the lack of PWHT which would improve the overall microstructural and mechanical properties to the levels of the base metal. Fig. 9 illustrate the hardness profiles produced for each sample. These plots indicate the change in the 10CrMo9-10 steel's response to the welding processes applied.

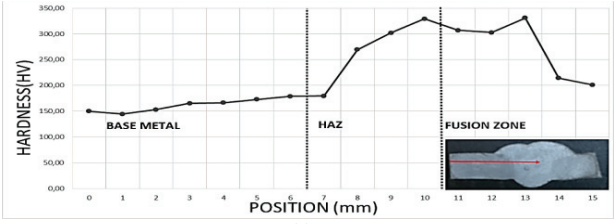

(a)

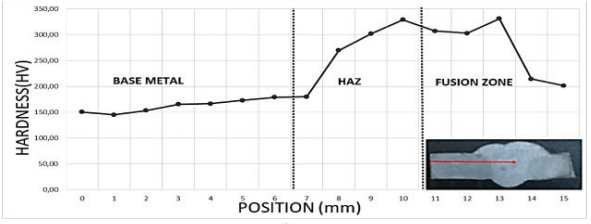

(b)

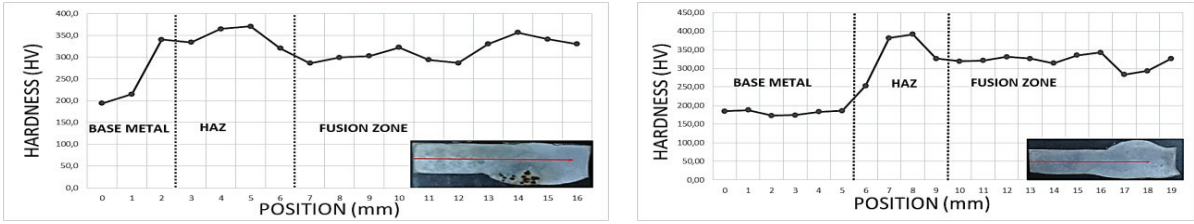

Fig. 9. Hardness profiles (a) Sample one (b) Sample two (c) Sample three (d) Sample four

3.4 P91 Microhardness and Tensile Strength

The minimum and maximum hardness and tensile strength results of the P91 sample are presented in Table 7. The base metal hardness remained in the range 200-250 HV, typical for P91 with a tensile strength also conforming to the range of 630-860 MPa.

Table 7. P91 minimum and maximum hardness and tensile strength values at different heights

	Hardness (HV)		Tensile Strength (MPa)	
Position (mm)	Min	Max	Min	Max
0	213	298	699	941
15	242	306	768	961
30	240	302	764	952
45	232	315	776	997
60	240	309	770	968

The P91 HAZ hardness measurements were in the range of 290-330 HV, while the tensile strength values remained below 1000 MPa showing the effectiveness of PWHT. An exception to the high hardness trend in the HAZ was seen in the FGHAZ region which recorded values lower than the base metal. The FGHAZ region may experience a softening resulting in hardness lower than the base metal because it does not experience heat input high enough to dissolve precipitates that will increase hardness. The CGHAZ region, however, dissolves precipitates leading the high hardness in the CGHAZ [12] (See recorded values at 15 and 30 mm in Fig. 10(a)).

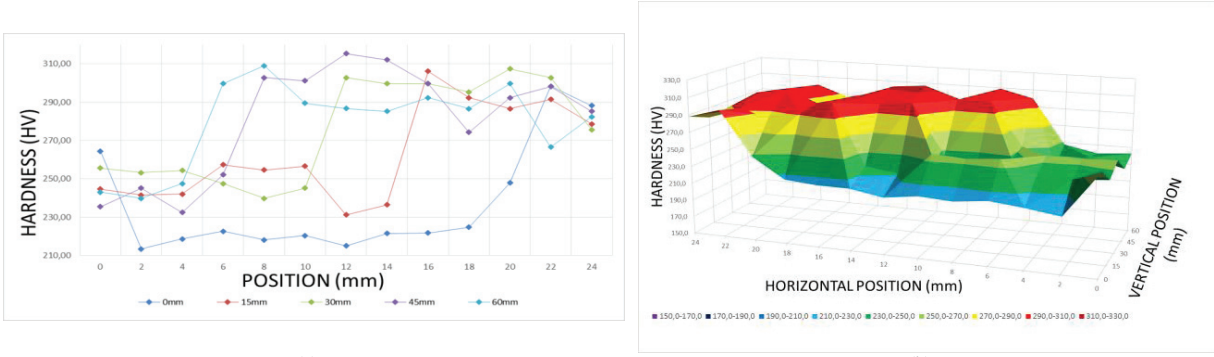

Fig. 10. (a) Combined P91 hardness profiles (b) P91 3D hardness profile

The most important observation that agrees with literature was that the FGHAZ would have lower hardness than the rest of the weldment regions due to the lack of precipitates at the FGHAZ grain boundaries implying that cracks could easily propagate through the HAZ, resulting in component failure. Fig. 10(b) shows a 3D distribution of the P91 hardness. The peak in hardness at the HAZ region of the weldment is clearly identified with the fusion zone

hardness being high but not as severe as the HAZ.

4. Conclusions

An investigation was successfully conducted on the effect of welding on the mechanical properties of P91 and 10CrMO9-10 creep resistance steels. Welded joints were produced by TIG and SMAW/MMA processes and examined using optical microscopy and micro hardness testing. The results obtained provided reasonable and realistic results that provided insight into the influence of welding processes on the mechanical properties of 10CrMo9-10 and P91 steels. The following conclusions could be made:

- The influence of heat input during welding significantly changed the microstructure of both investigation materials.
- The hardness results indicated that the HAZ would be a problematic area in the weldment because of the impact of heat input causing solid phase transformation in the HAZ resulting in high hardness and lower ductility.
- The fine grained heat affected zone (FGHAZ) which would have lower precipitate dissolution at the grain boundaries would experience a softening and reduction in creep resistance
- The tensile strength estimations from the micro hardness test results for the 10CrMo9-10 and P91 samples indicated that the base metals were in the acceptable range for the materials, but the HAZ region would cause a significant increase in hardness and tensile strength compromising material ductility and toughness.

Acknowledgements

Sample materials were provided by Eskom and welding was conducted at the Eskom Training School.

References

[1] J. Hilkes and V. Gross, “Welding CrMo Steels for Power Generation and Petrochemical Applications - Past, Present and Future,” *Bulletin of the Institute of Welding,* vol. 57, no. 2, pp. 11-22, 2013.

[2] S. Pant and S. Bhardwaj, “Properties and Welding Procedure for Grade 91 Alloy Steel,” *International Journal of Engineering Research and Technology.,* vol. 6, no. 6, pp. 767-772, 2013.

[3] P. J. Ennis and A. Czyrska-Filemonowicz, “Recent advances in creep-resistant steels for power plant,” *Sadhana,* vol. 28, no. 3-4, pp. 709-730, 2003.

[4] W. F. Newell Jr, “Welding and Postweld Heat Treatment of P91 Steels,” *Welding Journal,* vol. 89, no. 4, pp. 33-36, 2010.

[5] M. Abd El-Azim, O. Ibrahim and O. E. El-Desoky, “Long term creep behaviour of welded joints of P91 steel at 650 C,” *Materials Science & Engineering A,* vol. 560, no. 26, p. 678–684, 2013.

[6] K. K. Coleman and W. F. Newell Jr., “P91 and Beyond,” *Weld Journal,* vol. 86, no. 88, pp. 29-33, 2007.

[7] D. G. Robertson, “Traditional low alloy steels in power,” in *Coal Power Plant Materials and Life Assessment: Developments and Applications*, Sawston, Elsevier,, 2014, pp. 107-126.

[8] J. C. Vaillant, B. Vandenberghe, B. Hagn, H. Heuser and C. Jochum, “T/P23, 24, 911 and 92: New grades for advanced coal-fired power plants—Properties and experience,” *International Journal of Pressure Vessels and Piping,* vol. 85, no. 1-2, pp. 38-46, 2008.

[9] A. Al-Mazrouee, R. K. Singh Raman and R. N. Ibrahim, “Effect of post weld heat treatment on the oxide scaling of Cr–Mo steel weldments,” *Journal of Materials Processing Technology,* Vols. 164-165, p. 964–970, 2005.

[10] C. R. Das, S. K. Albert, A. K. Bhaduri, G. Srinivasan and B. S. Murty, “Effect of prior microstructure on microstructure and mechanical properties of modified 9Cr–1Mo steel weld joints,” *Materials Science and Engineering: A,* vol. 477, no. 1-2, pp. 185-192, 2008.

[11] M. Divya, C. R. Das, S. K. Albert, S. Goyal, P. Ganesh, R. Kaul, J. Swaminathan, B. S. Murty, L. M. Kukreja and A. K. Bhaduri, “Influence of welding process on Type IV cracking behavior of P91steel,” *Materials Science & Engineering :A,* vol. 613, pp. 148-158, 2014.

[12] S. Paddea, J. A. Francis, A. M. Paradowska, P. J. Bouchard and I. A. Shibli, “Residual stress distributions in a P91 steel-pipe girth weld before and after post weld heat treatment,” *Materials Science and Engineering A,* vol. 534, p. 663– 672, 2012.